

1 **Electric field variability and classifications of Titan's magnetoplasma**
2 **environment**

3

4 C.S. Arridge^{1,2}, N. Achilleos^{3,2}, P. Guio^{3,2}

5 1. Mullard Space Science Laboratory, University College London, Dorking, RH5 6NT, UK.

6 2. The Centre for Planetary Sciences at UCL/Birkbeck, Gower Street, London, WC1E 6BT,
7 UK.

8 3. Department of Physics and Astronomy, University College London, Gower Street,
9 London, WC1E 6BT.

10

11 Running Title: Convection electric field upstream of Titan

12

13 Keywords: Magnetosphere interactions with satellites and rings; Planetary magnetospheres;

14 Electric fields

15

15 Abstract

16 The atmosphere of Saturn's largest moon Titan is driven by photochemistry, charged particle
17 precipitation from Saturn's upstream magnetosphere, and presumably by the diffusion of the
18 magnetospheric field into the outer ionosphere, amongst other processes. Ion pickup,
19 controlled by the upstream convection electric field, plays a role in the loss of this
20 atmosphere. The interaction of Titan with Saturn's magnetosphere results in the formation of
21 a flow-induced magnetosphere. The upstream magnetoplasma environment of Titan is a
22 complex and highly variable system and significant quasi-periodic modulations of the plasma
23 in this region of Saturn's magnetosphere have been reported. In this paper we quantitatively
24 investigate the effect of these quasi-periodic modulations on the convection electric field at
25 Titan. We show that the electric field can be significantly perturbed away from the nominal
26 radial orientation inferred from Voyager 1 observations, and demonstrate that upstream
27 categorisation schemes must be used with care when undertaking quantitative studies of
28 Titan's magnetospheric interaction, particularly where assumptions regarding the orientation
29 of the convection electric field are made.

30

31

32 1. Introduction

33 Titan is Saturn's largest moon and the only moon in the solar system known to have a thick
34 atmosphere with an extended exosphere. The formation of Titan's flow-induced
35 magnetosphere is the only known case in the solar system where an essentially
36 unmagnetised body with a thick atmosphere interacts with a magnetospheric plasma. The
37 atmosphere is driven by photochemistry, by charged particle precipitation from the upstream
38 magnetosphere, and presumably by the diffusion of the magnetospheric field into the outer
39 ionosphere. The development of accurate models of the dynamical structure, chemistry,
40 formation and mass loss of Titan's atmosphere rely on an accurate knowledge and
41 characterisation of the local magnetoplasma environment, in order to constrain external
42 sources of energy for the system. See Arridge et al. (submitted manuscript, 2011a) for a
43 review of Titan's upstream plasma environment.

44

45 The upstream magnetoplasma environment of Titan is a complex and highly variable system
46 and is modulated by internal magnetospheric effects, including apparent longitudinal
47 asymmetries, and external forcing by the solar wind. At Titan's orbital distance (semi-major
48 axis = 1.22×10^6 km = $20.27 R_S$ where $1 R_S = 60268$ km) the observed magnetic field can
49 become radially stretched at locations just outside Saturn's magnetodisc current sheet, itself a
50 principal external field source (Arridge et al., 2008c). Vertical motions of this magnetodisc
51 (Arridge et al., 2008a; Bertucci et al., 2009; Simon et al., 2010a) can place Titan alternately
52 inside this current sheet or in the lobe-type regions adjacent to the sheet, which are relatively
53 devoid of plasma. The plasma is centrifugally confined in this magnetodisc whereas the
54 energetic particles are more free to extend to higher latitudes (e.g., Achilleos et al., 2010;

55 Sergis et al., in press). A number of authors have attempted to classify the upstream
56 environment of Titan (Rymer et al., 2009; Simon et al., 2010a; Garnier et al., 2010) using a
57 variety of criteria to produce categories such as “plasma sheet” or “current sheet” or “lobe”.
58 The classifications have proven to be useful in understanding flyby-to-flyby variability of
59 Titan’s atmosphere (e.g., Westlake et al., 2011). However, such classifications necessarily
60 produce a relatively coarse description of the upstream environment, which does not reduce
61 their value but emphasises that care must be applied in their use, especially for quantitative
62 studies.

63

64 Two examples highlight the need for caution. Firstly, energetic neutral atom (ENA)
65 observations can be used to perform remote sensing of Titan’s electromagnetic field
66 environment. However, the models used to interpret these observations show that the
67 morphology of the ENA fluxes are highly sensitive to the electric and magnetic field
68 environment of Titan (e.g. Wulms et al. 2010). Hence, making an assumption regarding the
69 electric field orientation and its stationarity based on a categorisation might introduce errors
70 into the interpretation of the ENA observations. As a second example, let us consider the
71 motion of pickup ions produced from Titan’s exosphere. Under a “nominal” radial convection
72 electric field orientation pickup ions will be directed away (towards) Titan on the anti-
73 Saturnward (Saturnward) side. However, when the electric field is oriented north-south pickup
74 ion trajectories are in the plane formed by Titan’s spin axis and the upstream plasma flow
75 direction. This not only changes the region of velocity space one should search for pickup
76 ions but also can change the location in Titan’s atmosphere where pickup ions are deposited
77 thus changing the location of sputtering and heating processes in the thermosphere (e.g,
78 Sittler et al., 2009; Johnson et al., 2009; and references therein). If the electric field magnitude
79 were also to change then this might also increase the magnitude of any atmospheric loss due
80 to pickup.

81

82 During the Voyager 1 flyby of Titan the convection electric field was thought to be directed
83 radially away from Saturn because the plasma flows azimuthally past Titan and the
84 background magnetic field was orientated north-south. Cassini studies of the regions
85 upstream of Titan have shown that the magnetic field there is very frequently in a radial
86 orientation (Arridge et al., 2008c; Bertucci et al., 2009; Simon et al., 2010a). It can also be
87 highly variable, changing from a north-south orientation to a radial orientation over timescales
88 of less than one hour (Arridge et al., 2008a; Simon et al., 2010b). These sudden variations in
89 the orientation of the magnetic field can produce significant and rapid rotations in the
90 orientation of the convection electric field in Titan’s rest frame.

91

92 In this letter we explore the effect of such variability in the upstream magnetic field and
93 quantify the associated variability in the convection electric field. We refer these results to
94 previously established classification schemes and show that classifying Titan’s upstream

95 environment as “current-sheet” does not guarantee a particular orientation of the electric field.
 96 These results are therefore of relevance in trying to understand the dynamics and evolution of
 97 Titan’s atmosphere (e.g., Johnson et al., 2009; Sittler et al., 2009) and for interpreting
 98 spacecraft data near Titan (e.g., Simon et al., 2007).

101 2. Modelling variations in the convection electric field

102 We consider the time-dependent variations of the convective electric field \mathbf{E} in Titan’s rest
 103 frame. We work throughout in cylindrical coordinates aligned with the current/plasma sheet
 104 but assume that the sheet is minimally distorted during its flapping motion such that the unit
 105 vectors may be defined as follows: \mathbf{e}_ρ is nearly radially outward from Saturn and lies precisely
 106 in the plane of the moving plasma sheet, \mathbf{e}_z is nearly parallel to Saturn’s spin axis and
 107 orthogonal to the plane of the sheet, and \mathbf{e}_ϕ is parallel to the corotation direction. In this frame
 108 the z coordinate of Titan may vary considerably as the current/plasma sheet oscillates about
 109 the kronographic equator.

111 Starting with the definition of \mathbf{E} and assuming zero radial flow for the magnetospheric plasma
 112 one finds the following components of the electric field as measured in the rest frame of Titan:

$$114 \quad E_\rho = u_z B_\phi - u_\phi B_z \quad E_\phi = -u_z B_\rho \quad E_z = u_\phi B_\rho \quad (1)$$

116 In this expression (E_ρ , E_ϕ , E_z) and (B_ρ , B_ϕ , B_z) are the electric and magnetic field
 117 components in cylindrical coordinates. The azimuthal component of the plasma velocity, u_ϕ is
 118 measured in Titan’s reference frame (the plasma speed less Titan’s orbital speed of ~ 5.6 km
 119 s^{-1}) and u_z is the axial (north-south) speed of the plasma/current sheet. Therefore we recover
 120 the pre-Cassini radial electric field ($E_\rho = -u_\phi B_z$) with a modification introduced by vertical
 121 plasma flow in the presence of an azimuthal field component, this vertical plasma flow also
 122 introduces an azimuthal electric field when combined with a radial field. The azimuthal plasma
 123 flow and radial field then combine to produce the axial electric field. The presence of a radial
 124 component in the magnetic field essentially produces a convection electric field which is non-
 125 radial – a stronger B_ρ and more rapid azimuthal plasma flow produces a larger axial electric
 126 field, and a strong B_ρ and more rapid axial flow produces a larger azimuthal electric field.

128 One can now ask what the total time derivative of \mathbf{E} is at Titan as a result of the motion of the
 129 plasma sheet and how it might change with the controlling parameters in Saturn’s
 130 magnetosphere. Figure 1 illustrates the theoretical setup with three configurations. Consider
 131 the plasma and current sheet to be in almost constant axial motion at a speed u_z . Because

132 the plane of Titan's orbit is close to Saturn's equatorial plane Titan will appear to move with
 133 respect to an observer in the co-moving frame of the plasma sheet. At any given time, Titan
 134 may be located at some particular position with respect to this current sheet; it may be located
 135 above, in, or below the centre-plane of the sheet. To determine the time derivative of the
 136 electric field in Titan's rest frame we need to evaluate the total derivative $D\mathbf{E}/dt = \partial\mathbf{E}/\partial t - u_z d\mathbf{E}/dz$
 137 where the negative sign has been introduced to account for the fact that when the plasma
 138 sheet is moving up with $u_z > 0$ Titan is actually moving down through the plasma sheet. We
 139 assume that the electric field at a fixed point in the sheet to be constant hence $\partial\mathbf{E}/\partial t = 0$ and
 140 the total derivative then reduces to the convective derivative associated with the relative
 141 motion of the plasma sheet and satellite.

142

143 We write the total derivative $D\mathbf{E}/Dt = -u_z d\mathbf{E}/dz$ and replace the spatial derivative of the
 144 azimuthal plasma speed with $(\partial u_\phi / \partial L)(\partial L / \partial z)$ as the product of the equatorial velocity shear of
 145 the azimuthal plasma flow, and the stretching of the magnetic field (a more highly stretched
 146 field will result in a larger derivative $\partial L / \partial z$) where L is the L-shell of the magnetic field line
 147 (defined here as the equatorial radial distance where the magnetic field line crosses the
 148 equator). Here we use Ferraro's isorotation theorem (Ferraro, 1937) to write $u_\phi = u_\phi(L)$ where
 149 $L = L(\rho, z)$ implying that the plasma on a given field line moves at the same azimuthal velocity.
 150 Note that $\partial u_z / \partial z$ is set to zero implying that the axial speed of the plasma sheet does not
 151 change across the height of the plasma sheet. Applying this formalism and using these
 152 assumptions we find:

153

$$\begin{aligned} \frac{DE_\rho}{Dt} &= u_z \left[B_z \frac{\partial u_\phi}{\partial L} \frac{\partial L}{\partial z} + u_\phi \frac{\partial B_z}{\partial z} - u_z \frac{\partial B_\phi}{\partial z} \right] \\ \frac{DE_\phi}{Dt} &= u_z^2 \frac{\partial B_\rho}{\partial z} \\ \frac{DE_z}{Dt} &= -u_z \left[B_\rho \frac{\partial u_\phi}{\partial L} \frac{\partial L}{\partial z} + u_\phi \frac{\partial B_\rho}{\partial z} \right] \end{aligned} \quad (2)$$

155

156 Hence we can see that there is a strong dependence of the time derivative of the convection
 157 electric field on how quickly the azimuthal velocity varies with L (velocity shear, $\partial u_\phi / \partial L$), how
 158 stretched the field is ($\partial L / \partial z$) and of course how rapidly the plasma sheet is moving in the axial
 159 direction (u_z). There is also a dependence on the vertical acceleration of the plasma sheet.
 160 Hence in a highly stretched magnetodisc with a large velocity shear and intense flapping one
 161 can expect rapid changes in the convection electric field strength and direction. We show the
 162 azimuthal component for completeness and do not discuss it further since not only is E_ϕ the
 163 smallest electric field component but its derivative is also the smallest. All of these quantities
 164 must be evaluated at the coordinates (ρ, ϕ, z) of Titan in the plasma sheet coordinate frame.

165

166 To estimate the magnitudes of such temporal modulation of the convection electric field we
 167 have used a self-consistent Euler potential model of Saturn's magnetospheric plasma and
 168 current sheet (Achilleos et al. 2010). Because this Euler potential model does not contain
 169 azimuthal fields we have assumed that $B_\phi = -0.5B_p$ but the exact value of this proportionality
 170 does not significantly affect our conclusions. This estimate is obtained from the sweepback
 171 angles in Bertucci et al. (2009) and Fig 1. of Arridge et al. (2008a). We couple this with an
 172 empirical structural model for the flapping of Saturn's plasma and current sheet (Arridge et al.,
 173 submitted manuscript, 2011b).

174

$$175 \quad z_{CS}(t, \varphi, \rho) = \left[\rho - r_H \tanh\left(\frac{\rho}{r_H}\right) \right] \tan \theta_{SUN} + (\rho - \rho_0) \tan \theta_{TILT} \cos \Psi_{PS}(t, \varphi, \rho) \quad (3)$$

176

177 This "wavy magnetodisc" model (3) gives the vertical position of the plasma sheet as a
 178 function of time and radial distance, from which u_z can be easily computed. In this expression,
 179 r_H , θ_{SUN} , ρ_0 , and θ_{TILT} are constants which are obtained by fitting the model to data, and Ψ_{PS} is
 180 a phase function which is a function of time (varying between 0 and 2π over one
 181 "magnetospheric period", equal to $2\pi/\Omega$), local time φ , time t , and radial distance ρ .

182

183 Because this is time-dependent it can be differentiated to give the vertical speed u_z of the
 184 plasma sheet (4) required to calculate (2). In this derivative the "DC" warping term (Arridge et
 185 al., 2008b) from (3) is a constant and becomes zero. The maximum speed of this current
 186 sheet is obtained when $\Psi_{PS} = 90^\circ$ and maximum acceleration when $\Psi_{PS} = 0^\circ$. We use values of
 187 $\rho_0 = 12 R_S$ and $\theta_{TILT} = 12^\circ$ as obtained by Arridge et al. (submitted manuscript, 2011b). Using
 188 these values at Titan's orbital distance we find $u_z(\Psi_{PS} = 90^\circ) = 17 \text{ km s}^{-1}$. In this expression,
 189 $\Omega = d\Psi_{PS}/dt$ is the angular frequency of Saturn's global magnetospheric oscillations.

190

$$191 \quad u_z(t, \varphi, \rho) = -(\rho - \rho_0) \Omega \tan \theta_{TILT} \sin \Psi_{PS}(t, \varphi, \rho) \quad (4)$$

192

193

194 3. Results

195 In figure 2 we present the magnetic field profile through the current sheet from the Euler
 196 potential model and the calculated convection electric fields. As expected from (1) only the
 197 radial and azimuthal electric field components exhibit any dependence on the speed of the
 198 sheet, between maximum and zero speed cases, due to the presence of u_z in these
 199 expressions. In each case the effect is fairly modest between the static and moving current
 200 sheet cases. Note that these have been plotted for the current sheet moving down over the
 201 spacecraft $u_z < 0$. For positive current sheet speeds the azimuthal and radial components are

202 reflected about the x axis. This is because the equations for E_ρ and E_φ are modulated by u_z
203 and swap sign when the plasma sheet is moving in a different direction.

204

205 The location of the current sheet/lobe boundary has been estimated from the criteria of Simon
206 et al. (2010a) where the current sheet is defined as $B_\rho \leq 0.6B$. To calculate \mathbf{B} we have
207 ignored the artificial B_φ introduced to solve equations (1) and (2) as this was not calculated
208 self-consistently; doing so results in an artificially large estimate of the current sheet
209 thickness. At the centre of the sheet the radial component dominates whereas at the
210 sheet/lobe boundary (indicated by the vertical dotted lines) the radial and axial electric field
211 components are roughly equal in magnitude, and in the lobes the axial component dominates.

212

213 In figure 3 the derivatives given by equations (2) are plotted. Because the derivatives are zero
214 when the current sheet is static we plot the case for the sheet moving down over the
215 spacecraft ($u_z < 0$, solid line) and moving up over the spacecraft ($u_z > 0$, dashed line). The curve
216 for DE_ρ/Dt is not precisely reflected about the x axis because of the u_z^2 term in (2). We
217 exclusively consider the $u_z < 0$ case (solid line) considering the consequences for Titan moving
218 up through the sheet (also see figure 1c).

219

220 At the centre of the current sheet near $z=0$ the electric field is radial and the largest derivative
221 is DE_z/dt consistent with $E_z > 0$ above the equator and $E_z < 0$ below the equator (odd-
222 symmetry). In the lobes outside of the vertical dotted lines (from the criteria of Simon et al.
223 (2010a)) the electric field derivatives are of a similar magnitude and are approximately 0.1 mV
224 $\text{m}^{-1} \text{ hour}^{-1}$. This is a substantial fraction of the magnitude of the convection electric field
225 showing that large rapid changes in \mathbf{E} occur over hour-long timescales. It is interesting to note
226 that within the current sheet E_z changes rapidly, reaching a significant fraction of its lobe field
227 value within the current sheet (see figure 2), whereas the largest changes in E_ρ are found
228 near the lobe. Consequently for a spacecraft located in the current sheet with the plasma
229 sheet moving rapidly over the spacecraft, large changes in E_z and rotations of up to 45° in the
230 orientation of \mathbf{E} will be found before the spacecraft has entered the lobe. This has important
231 consequences for the classification of Titan's upstream environment where although the
232 upstream environment may be jointly classified as current sheet (e.g., Simon et al. 2010a)
233 and plasma sheet (e.g., Rymer et al. 2009), which might lead to assumptions regarding the
234 orientation of the convection electric field, the orientation of this field may be highly non-
235 stationary. In such circumstances the use of these criteria may affect studies which make
236 assumptions about the orientation and magnitude of \mathbf{E} , for example the interpretation of ENA
237 observations (e.g., Wulms et al. 2010), pickup ion trajectories and subsequent ionospheric
238 heating and loss (e.g. Sittler et al., 2009; Johnson et al. 2009; and references therein), and
239 modelling of the orientation of the induced magnetotail, and modelling ionospheric currents,
240 ionospheric heating and the thermosphere (e.g., Cravens et al. 2009; Ågren et al. 2010).

241

242 The total time derivative of E_z is completely dominated by the second term on the right-hand-
243 side, $u_\phi \partial B_\phi / \partial z$, due to the rapid azimuthal plasma speed and the large vertical gradients in the
244 radial field produced by the current sheet. The shear in the azimuthal plasma velocity (∂u_ϕ
245 $/ \partial L$) was found to be fairly small thus contributing to the small magnitude of the first term.
246 Similarly the total time derivative of the E_ϕ is dominated by the $u_\phi \partial B_z / \partial z$ term even though the
247 vertical gradients in B_z are relatively small. The next important term is the $u_z \partial B_\phi / \partial z$ term and is
248 smaller than the $u_\phi \partial B_z / \partial z$ term because the axial speed of the plasma sheet is much smaller
249 than the azimuthal convection speed of Saturn's magnetospheric plasma (17 km s^{-1} Vs. ~ 120
250 km s^{-1}) and the radial component of the magnetic field is larger than the azimuthal
251 component.

252

253

254 4. Conclusions

255 In this paper we have theoretically examined the effects of magnetodisc flapping on the
256 convection electric field at Titan. We have found that even when classification schemes place
257 Cassini in the current sheet near a Titan flyby, which might indicate a radial electric field,
258 there may in fact be an equally important north-south component. Users of classification
259 schemes must be aware that such modulations might not be captured by these schemes.
260 However, it is important to note that this does not devalue methods for classifying Titan's
261 plasma environment but does highlight the need for caution in their use, particularly for
262 quantitative studies.

263

264 The picture of a quasi-static upstream environment where either the spacecraft is in a
265 constant homogeneous lobe or current sheet field configuration does not appear to be valid in
266 the Cassini era (e.g., Arridge et al., 2008b, 2008c; Bertucci et al., 2009; Simon et al.,
267 2010a, 2010b; Arridge et al., submitted manuscript, 2011b), possibly as a result of seasonal
268 forcing on Saturn's magnetosphere or particular magnetospheric conditions encountered by
269 Voyager 1. The picture now emerging from various studies is that of a current and plasma
270 sheet in constant motion, with both long (near the planetary rotation period) and short period
271 (due to magnetospheric dynamics driven by internal processes and solar wind variability)
272 motions. This study identifies and classifies the different sources and controlling parameters
273 for the dynamics and variability of the convective electric field.

274

275 Further work is required to address the consequences of such rapid changes in the electric
276 field on Titan's induced magnetosphere, ionosphere and atmosphere.

277

278

279

280 **Acknowledgements**

281 CSA thanks Nick Sergis and the referee for useful comments on the manuscript. CSA was in
282 this work by a Science and Technology Facilities Council Postdoctoral fellowship (under grant
283 ST/G007462/1), the Europlanet RI project (under grant number 228319), and the International
284 Space Science Institute. CSA thanks staff at the International Space Science Institute for their
285 hospitality during a meeting where this work was first presented. We thank the many
286 individuals at JPL, NASA, ESA and numerous PI and Co-I institutions who have contributed to
287 making the Cassini project an outstanding success.

288

289

290

291 **References**

292

293 N. Achilleos, P. Guio, C.S. Arridge, A model of force balance in Saturn's magnetodisc,
294 MNRAS, 401(4), 2349-2371, doi:10.1111/j.1365-2966.2009.15865.x (2010).

295

296 K. Ågren, D.J. Andrews, S.C. Buchert, A.J. Coates, S.W.H. Cowley, M.K. Dougherty, N.J.T.
297 Edberg, P. Garnier, G.R. Lewis, R. Modolo, H. Opgenoorth, G. Provan, L. Rosenqvist, D.L.
298 Talboys, J.-E. Wahlund, and A. Wellbrock, Detection of currents and associated electric
299 fields in Titan's ionosphere from Cassini data, J. Geophys. Res., 116, A04313,
300 doi:10.1029/2010JA016100 (2011).

301

302 C.S. Arridge, N. André, N. Achilleos, K.K. Khurana, C.L. Bertucci, L.K. Gilbert, G.R. Lewis,
303 A.J. Coates and M.K. Dougherty, Thermal electron periodicities at 20 R_S in Saturn's
304 magnetosphere, Geophys. Res. Lett., 35, L15107, doi:10.1029/2008GL034132 (2008a).

305

306 C.S. Arridge, K.K. Khurana, C.T. Russell, D.J. Southwood, N. Achilleos, M.K. Dougherty, A.J.
307 Coates and H.K. Leinweber, Warping of Saturn's magnetospheric and magnetotail current
308 sheets, J. Geophys. Res., 113, A08217, doi:10.1029/2007JA012963 (2008b).

309

310 C.S. Arridge, C. T. Russell, K. K. Khurana, N. Achilleos, S. W. H. Cowley, M. K. Dougherty, D.
311 J. Southwood, E. J. Bunce, Saturn's magnetodisc current sheet. J. Geophys. Res. 113,
312 A04214, doi:10.1029/2007JA012540 (2008c).

313

314 C.S. Arridge, N. André, C.L. Bertucci, P. Garnier, C.M. Jackman, Z. Nemeth, A.M. Rymer, N.
315 Sergis, K. Szego, Upstream of Saturn and Titan, manuscript submitted to Space Sci. Rev.,
316 2011a.

317

318 C.S. Arridge, N. André, K.K. Khurana, C.T. Russell, S.W.H. Cowley, G. Provan, D.J.
319 Andrews, C.M. Jackman, A.J. Coates, E.C. Sittler, M.K. Dougherty, D.T. Young, Periodic
320 motion of Saturn's nightside plasma sheet, manuscript submitted to J. Geophys. Res., 2011b.

321

322 C. Bertucci, F.M. Neubauer, K. Szego, J.-E. Wahlund, A.J. Coates, M.K. Dougherty, D.T.
323 Young, W.S. Kurth, Structure of Titan's mid-range magnetic tail: Cassini magnetometer
324 observations during the T9 flyby, *Geophys. Res. Lett.*, 34, L24S02,
325 doi:10.1029/2007GL030865 (2007).

326

327 C. Bertucci, B. Sinclair, N. Achilleos, P. Hunt, M.K. Dougherty, C.S. Arridge (2009), The
328 variability of Titan's magnetic environment, *Planet. Space Sci.* 57(14-15), 1813-1820,
329 doi:10.1016/j.pss.2009.02.009 (2009).

330

331 T.E. Cravens, R.V. Yelle, J.-E. Wahlund, D.E. Shemansky and A.F. Nagy, Composition and
332 Structure of the Ionosphere and Thermosphere, in *Titan from Cassini-Huygens*, Chapter 11,
333 pp. 259-295, ed. R.H. Brown, J.-P. Lebreton, J. Hunter Waite, Springer Science+Business
334 Media (2009).

335

336 V.C. Ferraro, The non-uniform rotation of the Sun and its magnetic field, *MNRAS*, 97, 458
337 (1937).

338

339 P. Garnier, I. Dandouras, D. Toubanc, E.C. Roelof, P.C. Brandt, D.G. Mitchell, S.M. Krimigis,
340 N. Krupp, D.C. Hamilton, J.-E. Wahlund, Statistical analysis of the energetic ion and ENA
341 data for the Titan environment, *Planet. Space Sci.*, 58(14-15), 1811-1822,
342 doi:10.1016/j.pss.2010.08.009 (2010).

343

344 R.E. Johnson, O.J. Tucker, M. Michael, E.C. Sittler, H.T. Smith, D.T. Young, J.H. Waite, Mass
345 Loss Processes in Titan's Upper Atmosphere, in *Titan from Cassini-Huygens*, Chapter 15, pp.
346 373-392, ed. R.H. Brown, J.-P. Lebreton, J. Hunter Waite, Springer Science+Business Media
347 (2009).

348

349 A.M. Rymer, H.T. Smith, A. Wellbrock, A.J. Coates, D.T. Young, Discrete classification and
350 electron energy spectra of Titan's varied magnetospheric environment, *Geophys. Res. Lett.*
351 36, L15109, doi:10.1029/2009GL039427 (2009).

352

353 N. Sergis, C.S. Arridge, S.M. Krimigis, D.G. Mitchell, A.M. Rymer, D.C. Hamilton, N. Krupp,
354 M.K. Dougherty, A.J. Coates, Dynamics and seasonal variations in Saturn's magnetospheric
355 plasma sheet, as measured by Cassini, *J. Geophys. Res.*, doi:10.1029/2010JA016180, in
356 press.

357

358 S. Simon, A. Boesswetter, T. Bagdonat, U. Motschmann, J. Schuele, Three-dimensional
359 multispecies hybrid simulation of Titan's highly variable plasma environment, *Ann. Geophys.*,
360 25, 117-144 (2007).

361

362 S. Simon, F.M. Neubauer, C.L. Bertucci, H. Kriegel, J. Saur, C.T. Russell, and M.K.
 363 Dougherty, Titan's highly dynamic magnetic environment: A systematic survey of Cassini
 364 magnetometer observations from flybys TA–T62, *Planet. Space Sci.*, 58(10), 1230-1251,
 365 doi:10.1016/j.pss.2010.04.021 (2010a).

366

367 S. Simon, A. Wennmacher, F.M. Neubauer, C.L. Bertucci, H. Kriegel, C.T. Russell, M.K.
 368 Dougherty, Dynamics of Saturn's magnetodisk near Titan's orbit: Comparison of Cassini
 369 magnetometer observations from real and virtual Titan flybys, *Planet. Space Sci.*, 58(12),
 370 1625-1635, doi:10.1016/j.pss.2010.08.006 (2010b).

371

372 E.C. Sittler, R.E. Hartle, C. Bertucci, A.J. Coates, T.E. Cravens, I. Dandouras, D. Shemansky,
 373 Energy Deposition Processes in Titan's Upper Atmosphere and Its Induced Magnetosphere,
 374 in *Titan from Cassini-Huygens*, Chapter 16, pp. 393-453, ed. R.H. Brown, J.-P. Lebreton, J.
 375 Hunter Waite, Springer Science+Business Media (2009).

376

377 J. Westlake, J.M. Bell, J.H. Waite Jr., R.E. Johnson, J.G. Luhmann, K.E. Mandt, B.A. Magee,
 378 A.M. Rymer, Titan's thermospheric response to various plasma environments, *J. Geophys.*
 379 *Res.*, doi:10.1029/2010JA016251, in press.

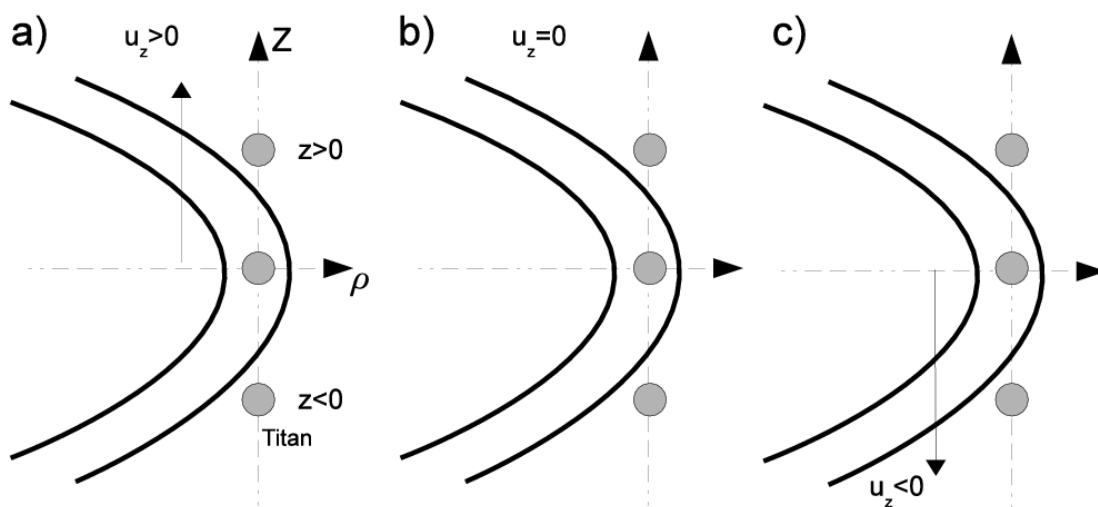
380

381 V. Wulms, J. Saur, D.F. Strobel, S. Simon, and D.G. Mitchell, Energetic neutral atoms from
 382 Titan: Particle simulations in draped magnetic and electric fields, *J. Geophys. Res.*, 115,
 383 A06310, doi:10.1029/2009JA014893 (2010).

384

385 **Figures**

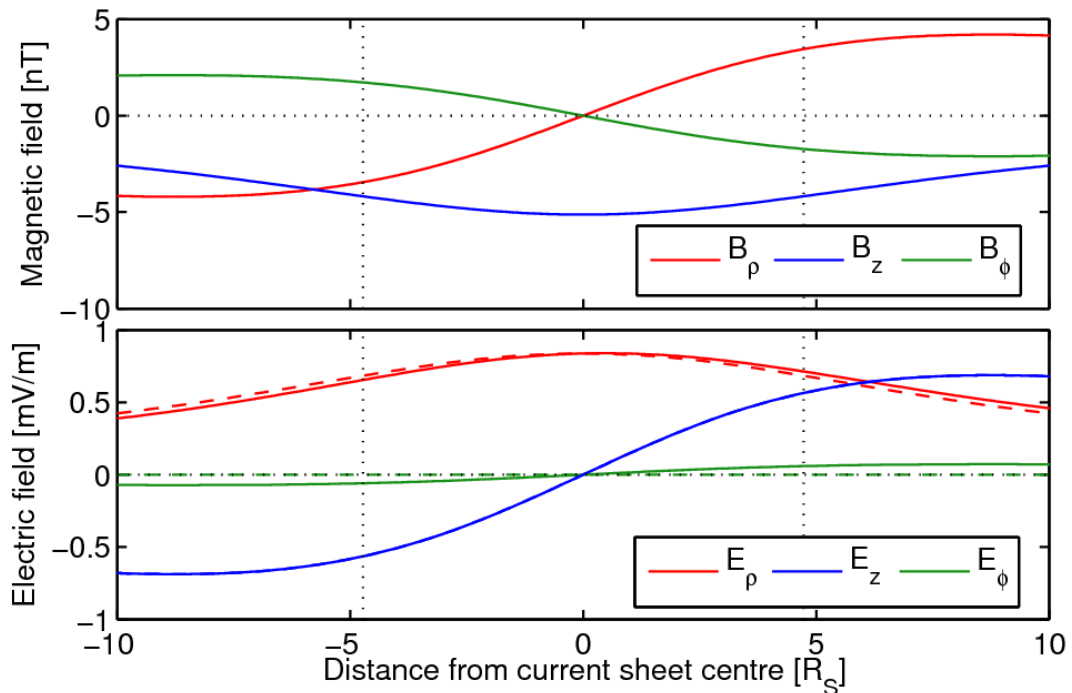
386

387 **Figure 1**

388

389 **Figure 1:** Illustration of the theoretical construction. The solid curves indicate magnetic field
 390 lines around a current sheet in the $z=0$ plane. The (z,ρ) coordinates indicate a convenient
 391 “sheet coordinate system”. Panel (a) shows the sheet moving upwards, (b) the sheet at rest,
 392 (c) the sheet moving downwards. In each case Titan (the grey circle) may be located above
 393 the sheet, near the centre of the sheet, or below the sheet. For example, the bottom circle in
 394 panel (b) would indicate Titan located below the sheet and the sheet at rest with respect to
 395 Titan. As a second example, the top circle in panel (a) would indicate Titan located above the
 396 sheet but with the sheet moving up to meet Titan, so Titan will shortly pass through the centre
 397 of the sheet.

398

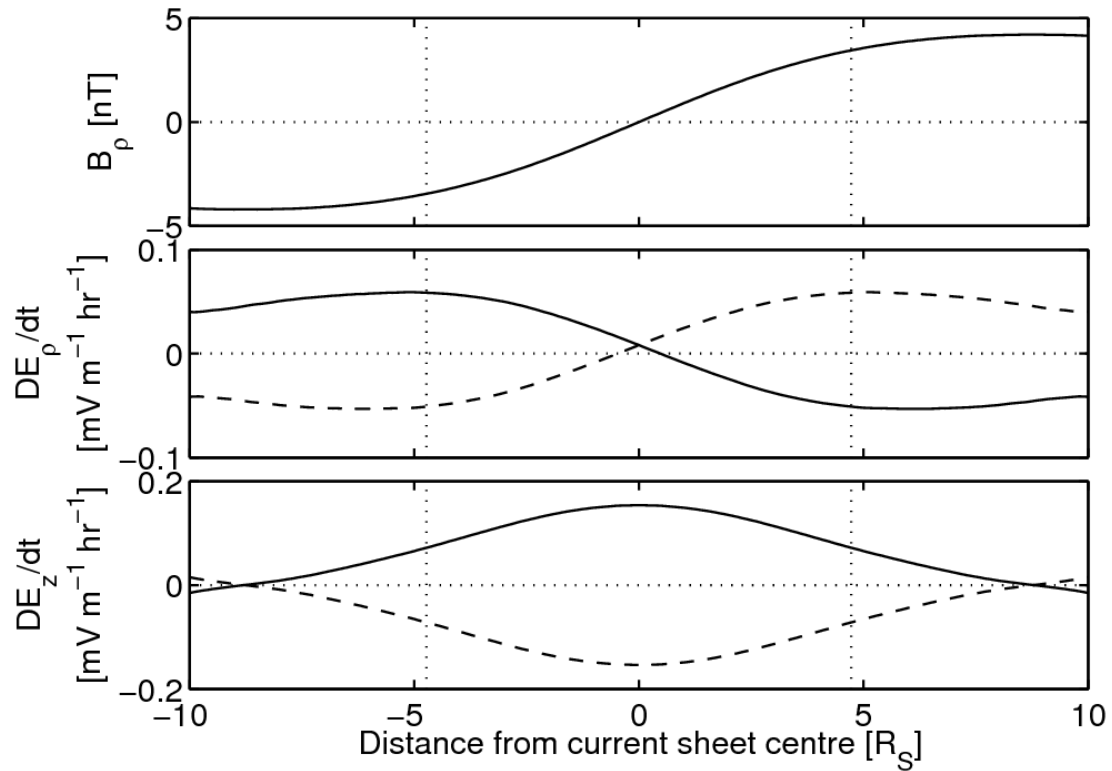
399 **Figure 2**

400

401 **Figure 2:** Calculated magnetic field profiles (top) and convection electric fields (bottom) as a
 402 function of axial distance from the centre of the current sheet, positive above the current
 403 sheet and negative below. In both panels red indicates the radial component, blue the axial,
 404 and green the azimuthal. The electric field is calculated for two cases i) where the current
 405 sheet is in rapid axial motion ($u_z \neq 0$) (solid lines) and ii) where the current sheet is at rest with
 406 respect to Titan ($u_z = 0$) (dashed lines). The dotted vertical lines indicate the extents of the
 407 current sheet as defined by the $B_\rho \leq 0.6B$ criterion of Simon et al. (2010a).

408

409 **Figure 3**



410

411 **Figure 3:** Calculated electric field derivatives as a function of axial distance from the centre of
 412 the current and plasma sheet. The top panel shows the radial component of the field for
 413 reference. The middle and bottom panels show the total time derivative of the radial and axial
 414 components of the electric field. The vertical dotted lines show the extents of the current
 415 sheet. The solid lines show the rate of change of the electric field when the sheet is in rapid
 416 axial motion downwards ($u_z < 0$) and the dashed line when the sheet is moving upwards ($u_z > 0$).
 417